

## Stimulated emission depletion nanoscopy of living cells using SNAP-tag fusion proteins

**Birka Hein, Katrin Willig, Christian A. Wurm, Volker Westphal, Stefan Jakobs, Stefan W. Hell**

### Angaben zur Veröffentlichung / Publication details:

Hein, Birka, Katrin Willig, Christian A. Wurm, Volker Westphal, Stefan Jakobs, and Stefan W. Hell. 2010. "Stimulated emission depletion nanoscopy of living cells using SNAP-tag fusion proteins." *Biophysical Journal* 98 (1): 158-63.  
<https://doi.org/10.1016/j.bpj.2009.09.053>.

# Stimulated Emission Depletion Nanoscopy of Living Cells Using SNAP-Tag Fusion Proteins

Birka Hein, Katrin I. Willig,\* Christian A. Wurm, Volker Westphal, Stefan Jakobs, and Stefan W. Hell\*

Max Planck Institute for Biophysical Chemistry, Department of NanoBiophotonics, Göttingen, Germany

**ABSTRACT** We show far-field fluorescence nanoscopy of different structural elements labeled with an organic dye within living mammalian cells. The diffraction barrier limiting far-field light microscopy is outperformed by using stimulated emission depletion. We used the tagging protein hAGT (SNAP-tag), which covalently binds benzylguanine-substituted organic dyes, for labeling. Tetramethylrhodamine was used to image the cytoskeleton (vimentin and microtubule-associated protein 2) as well as structures located at the cell membrane (caveolin and connexin-43) with a resolution down to 40 nm. Comparison with structures labeled with the yellow fluorescent protein Citrine validates this labeling approach. Nanoscopic movies showing the movement of connexin-43 clusters across the cell membrane evidence the capability of this technique to observe structural changes on the nanoscale over time. Pulsed or continuous-wave lasers for excitation and stimulated emission depletion yield images of similar resolution in living cells. Hence fusion proteins that bind modified organic dyes expand widely the application range of far-field fluorescence nanoscopy of living cells.

## INTRODUCTION

Far-field fluorescence microscopy is a powerful tool for the noninvasive imaging of protein distributions and dynamics in living cells (1). However, many structures within cells are too small to be resolved with standard light microscopes, whose resolution is restricted by diffraction to  $\sim 200$  nm in the lateral plane and to  $\sim 500$  nm in the axial direction (2). Several concepts are known by now that fundamentally overcome the diffraction barrier and allow the imaging of structures substantially  $< 100$  nm (3–5). In stimulated emission depletion (STED) microscopy (6–9), the fluorescence capability of the features located at the outer part of a scanning focal spot of excitation light is transiently switched off by prohibiting the population of their excited state through stimulated emission with a beam featuring a deep intensity minimum at the focal spot center. For improvement of the resolution in the focal plane, the STED beam is typically shaped into a doughnut that is superposed onto the excitation beam. Scanning the two co-aligned beams through the sample yields images with subdiffraction resolution. The achievable resolution depends on the spectral properties of the dye and the intensity of the STED light. Applying an intensity  $I$  at the doughnut crest reduces the fluorescent spot to a diameter  $d \cong \lambda/2NA\sqrt{1+I/I_s}$ , where  $I_s$  defines the STED beam intensity required to reduce the fluorescence probability to  $1/e$ . NA is the numerical aperture of the lens. The fact that  $I/I_s \rightarrow \infty$  leads to  $d \rightarrow 0$  indicates that the diffraction barrier is fundamentally overcome (10,11). More recent nanoscopy concepts utilize a transient switching of the individual fluorophores followed by mathematical localization (5,12–14).

All these approaches have been extended into the imaging of living cells, mostly using membrane dyes or various fluorescent proteins (FPs) as labels (7,15–17). FPs, which can be fused genetically to a protein of interest are attractive protein tags. However, due to the formation of the chromophore from several amino acids, their photophysical characteristics cannot be easily changed arbitrarily, and hence are not necessarily optimal for various nanoscopy approaches (18). Moreover, although many chemically synthesized fluorophores are superior to fluorescent proteins in photostability and quantum yield, one can rarely use them for specific protein labeling in living specimens.

During the past decade, innovative techniques were developed to append chemically synthesized fluorophores to proteins within living cells. Prominent examples include the biarsenical-tetracysteine system (19), the Halo-Tag (20), ACP- (21), and SNAP-tag (22) labeling approaches. The so-called SNAP-tag relies on human O6-alkylguanine-DNA alkyltransferase (hAGT) as a tag, which can be fused to a host protein. This tag has a size of 182 amino acids (aa), so it is slightly smaller than FPs ( $\sim 240$  aa). In its regular function, hAGT repairs DNA lesions resulting from the O6-alkylation of guanine by irreversibly transferring the alkyl group to a reactive cysteine of hAGT (23). This reaction is not limited to alkylated DNA but can be extended to benzylguanines (BG) and related compounds carrying different substituents at the 4-positions of the benzyl ring. Exploiting this reaction, hAGT has been used as a tag. In this case, the nucleotide-moiety of a fluorescent BG derivative is recognized by hAGT that is genetically fused to a host protein. A covalent bond is formed between the protein and the fluorophore, leading to a specific labeling of the protein of interest. It has been shown that hAGT fusion proteins can be specifically labeled in living cells by adding various fluorescent BG derivatives (22).

\*Correspondence: kwillig@gwdg.de or hell@nanoscopy.de

In this study, we labeled mammalian cells expressing various hAGT fusion proteins with the commercially available substrate TMR-Star, which is based on the red-emitting dye tetramethylrhodamine (TMR). Using this tag, we show an all-physics based resolution enhancement down to  $\sim 40$  nm using STED microscopy in living cells. Because this tagging strategy enables the labeling of intracellular proteins with a variety of different fluorophores, it facilitates new recording strategies for far-field fluorescence nanoscopy.

## MATERIAL AND METHODS

### Plasmid construction

Standard methods were used for cloning. To tag CAV1, Cx43 and vimentin at the C-terminus with hAGT, the expression plasmids pSEMS-CAV1-SNAP26m, pSEMS-GJA1-SNAP26m, and pSEMS-VIM-SNAP26m, were constructed by Gateway vector conversion (24)(Invitrogen, Carlsbad, CA) from the donor vector pDONR223-CAV1, pDONR223-GJA1, and pDONR223-VIM and the empty destination vector pSEMS-Gateway-SNAP26m (Covalys Biosciences, Witterswil, Switzerland). The microtubule-associated protein MAP2 was tagged at its N-terminus with hAGT. The respective plasmid was constructed by Gateway vector conversion from the donor vector pDONR223-MAP2 and the empty destination vector pSEMS-SNAP26m-Gateway (Covalys Biosciences). For tagging with the fluorescent protein Citrine, the coding sequence for hAGT was substituted with the respective Citrine-sequence.

### Cell culture and transfection

The mammalian PtK2 cell line was grown as previously described (16). For transfection, PtK2 cells were grown overnight on glass coverslips. After reaching  $\sim 80\%$  confluence, the plasmids were introduced using the Nanofectin kit according to the manufacturer's instructions (PAA, Pasching, Austria).

### Labeling

Twenty-four hours after transfection, cells were incubated for 15 min at  $37^\circ\text{C}$  in a freshly prepared solution of  $1 \mu\text{M}$  TMR-Star (Covalys), in Dulbecco's modified Eagle's medium (DMEM). Afterward, they were washed for 30 min in DMEM.

### STED microscopy

The STED microscopy setup was essentially as described previously (16). In brief, the STED focal doughnut was created by introducing a polymeric phase plate (RPC Photonics, Rochester, NY) applying a helical phase ramp of  $\exp(i\varphi)$ , with  $0 < \varphi < 2\pi$ , in the STED beam that was then focused into a 1.4 NA objective lens (PL APO,  $100\times$ , oil, Leica, Germany). Excitation and STED beams were overlapped and separated from the fluorescence by two custom-made dichroic mirrors. The fluorescence was filtered by

a 585/80 bandpass filter and imaged onto a multimode optical fiber with an opening of the size of about an Airy disc. Images were recorded with resonant mirror scanning (15 kHz, SC-30; EOPC, Glendale, NY) along the  $x$  axis and stage scanning along the  $y$  axis (P-733, Physik Instrumente, Karlsruhe, Germany). For imaging, the cells were transferred to a custom made sample holder using DMEM without phenol red as imaging medium. All images were recorded at  $24^\circ\text{C}$  within  $\sim 1$  h after removing the coverslip from the incubator.

## RESULTS

To evaluate STED microscopy on living cells labeled with hAGT, we first expressed connexin-43 (Cx43) fused to hAGT in PtK2 (potoroo kidney) cells. Cx43 is a ubiquitous member of the connexin family and is found in most mammalian tissues (25). It is a building block of gap junctions in the plasma membrane, which are essential for cell-to-cell communication. For labeling, we used the commercially available substrate TMR-Star (Fig. 1). This derivative features a photostable rhodamine as the fluorescent group with an excitation maximum at 554 nm and emission maximum at 580 nm. TMR-Star is cell-permeable, produces low unspecific fluorescence background, and exhibits low cellular toxicity. Images were recorded by exciting TMR with a pulsed laser diode at 532 nm and 80 MHz repetition rate (70 ps pulses, PicoTA; Toptica, Martinsried, Germany). For the STED image, the excitation was followed by STED pulses featuring a central wavelength  $\lambda_{\text{STED}} = 650$  nm, originating from an optical parametric oscillator (PP-OPO; APE, Berlin, Germany), which was pumped by a Ti:Sapphire laser (MaiTai; Spectra-Physics, Santa Clara, CA). The STED pulses were stretched by dispersion to a pulse length of  $\sim 300$  ps. A resonant beam scanner at 15 kHz was used for the fast scanning axis, rendering line scan durations of  $67 \mu\text{s}$ . To obtain a good signal/noise ratio, typically  $\sim 100$  lines were summed up when forming an image.

Fig. 2 A displays a confocal image of living PtK2 cells expressing Cx43 fusion protein, showing large clusters of  $\sim 200$  nm diameter on the plasma membrane. Finer substructures are blurred in the confocal recording but are resolved in the corresponding STED image (Fig. 2 B). Comparison shows that many adjacent small Cx43 clusters are discernible in the STED image but not in the corresponding confocal image (Fig. 2 C). For the STED imaging, the time-averaged power of the pulsed STED beam was 39 mW, corresponding to a peak intensity  $I = 882 \text{ MW/cm}^2$  of the STED pulse at the doughnut crest. To estimate the optical resolution, we

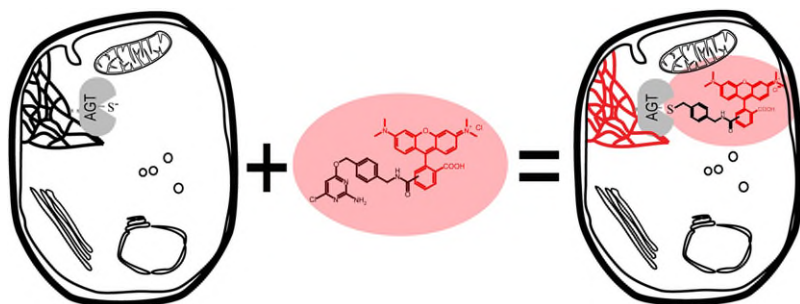


FIGURE 1 Schematic of the labeling approach used in this study: A fusion protein of the protein of interest and hAGT is expressed in the cell (left). On incubation, the substrate TMRStar diffuses through the membrane and binds covalently to hAGT, leading to a specific fluorescence labeling of the protein of interest.

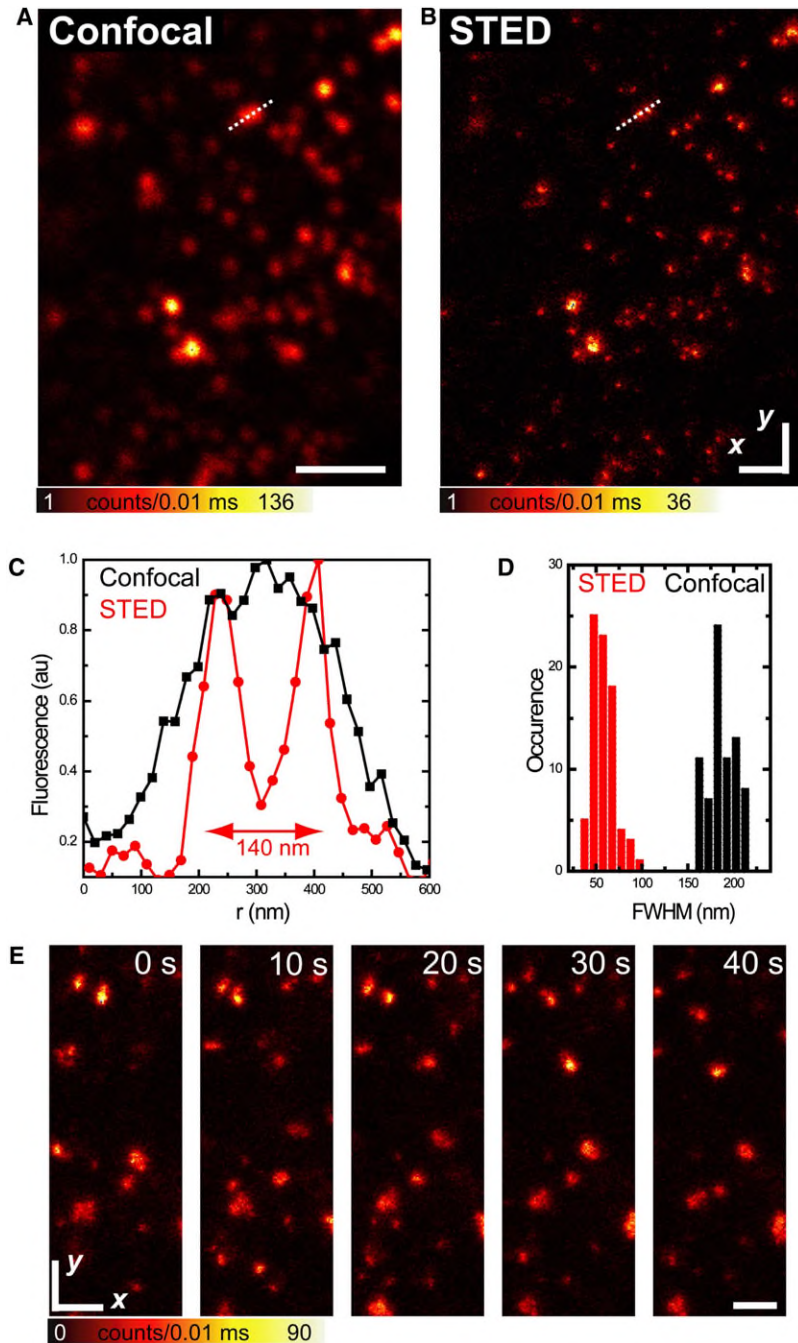


FIGURE 2 Subdiffraction-resolution STED imaging of gap junctions in living PtK2-cells. (A and B) Confocal and STED-image, respectively, of Connexin-43 fused to hAGT and labeled with TMR (raw data). Scale bar = 1  $\mu\text{m}$ . (C) Profiles along the marked line in A and B that show that individual clusters can be discerned by STED but are not separated by confocal microscopy. Considering the finite extent of the protein agglomerations, a histogram (D) of the FWHM of 74 measured line profiles through individual clusters indicates a resolution  $<40$  nm. (E) Time lapse STED imaging of the movement of Connexin-43 within the membrane. Scale bar = 500 nm.

determined the full-width-at-half-maximum (FWHM) of numerous individual Cx43 protein clusters labeled with TMR-Star in living cells by taking line profiles on 74 individual clusters and plotting the measured FWHMs in a histogram (Fig. 2 D). The distributions for the confocal and STED mode are well separated, showing that the size of the Cx43 clusters is well below the resolution limit of the confocal microscope. In the confocal mode, the resolution can be determined as the average of the measured confocal spot sizes that, in this case, amounts to 189 nm. This spot size is close to the theoretical limit as determined by diffraction. The smallest

FWHM values measured in the STED image indicate that a resolution down to 40 nm is achieved by this system under the applied conditions (Fig. 2 D). This value is in good agreement with simulations of the effective STED PSF for this fluorophore, when taking into account the measured TMR specific value for  $I_s = 36$  MW/cm<sup>2</sup> for 300 ps long pulses. FWHM values of up to 100 nm in the STED image reflect the broad cluster size distribution.

Next, we carried out time-lapse nanoscopy on cells expressing Cx43-hAGT labeled with TMR-Star. Ten frames with an acquisition time of 10 s per 20  $\mu\text{m} \times 20 \mu\text{m}$  frame

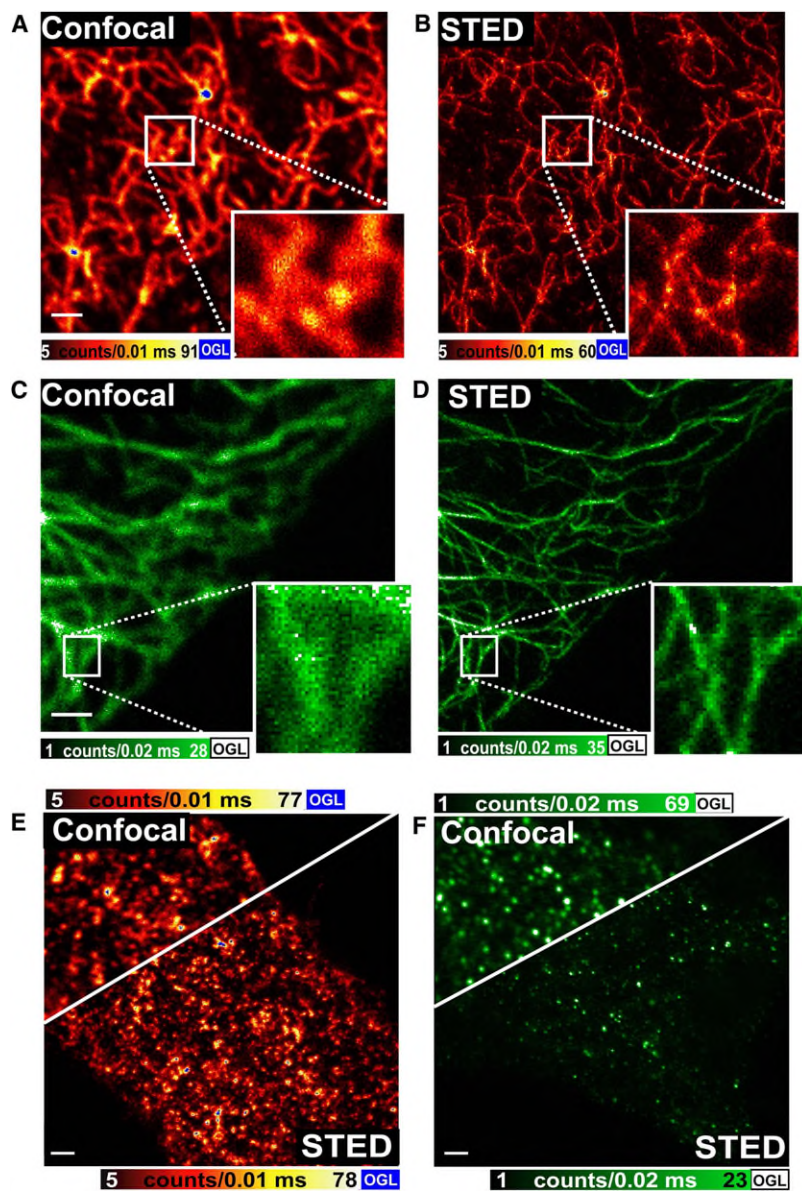


FIGURE 3 Comparison of labeling with the tagging protein hAGT and substrate TMR-Star versus labeling with the yellow fluorescent protein Citrine for live cell STED imaging. (A) Confocal versus (B) STED image of vimentin labeled with TMR via hAGT, showing that STED renders the vimentin network much more clearly than its confocal counterpart. (C and D) Analogous Citrine-fused structure. Caveolin labeled by TMR via hAGT is shown in E, whereas the data in F is recorded by labeling with Citrine. Again, in the STED part of the images, individual clusters can be resolved. All images display raw data that can be further processed by image deconvolution not applied here. Scale bars = 1  $\mu\text{m}$ .

were recorded. The first five STED images are shown in Fig. 2 E (see Movie S1 in the Supporting Material). Generally, in the STED mode, the fluorescence signal was reduced to half of its initial value after five to seven frames. The loss of fluorescence was compensated for by normalization of the maximal fluorescence intensity of the images in the movie.

To compare the performance of the hAGT approach with the use of fluorescent proteins as fluorescent markers in live cell STED microscopy, we created a vimentin fusion protein with hAGT and also with the fluorescent protein Citrine ( $\lambda_{\text{EM}} = 529 \text{ nm}$ ). Vimentin is a member of the intermediate filament family of proteins (26). These proteins build an extended cytoskeletal network in the cytoplasm. For STED imaging of Citrine, excitation at 490 nm was carried out, whereas  $\lambda_{\text{STED}} = 595 \text{ nm}$ .

The images of the cellular structures obtained after expression of vimentin-Citrine, or after vimentin-hAGT followed by labeling with TMR-Star are virtually identical. This result underscores that the staining procedure with TMR-Star does not interfere with cell integrity (Fig. 3, A and B). We find that for both vimentin-Citrine and vimentin-hAGT/TMR-Star, the STED microscope separates individual filaments, which tend to be blurred in the confocal image (Fig. 3, A and B). In fact, the resolution attained with the hAGT/TMR-Star labeling (40 nm) is slightly better than the 50 nm obtained for Citrine. Bleaching due to the STED beam is difficult to compare and quantify, because it also depends on the excitation power that has to be adapted to the brightness of each sample. In any case, the general observation was that more STED images can be recorded using TMR as a fluorophore.

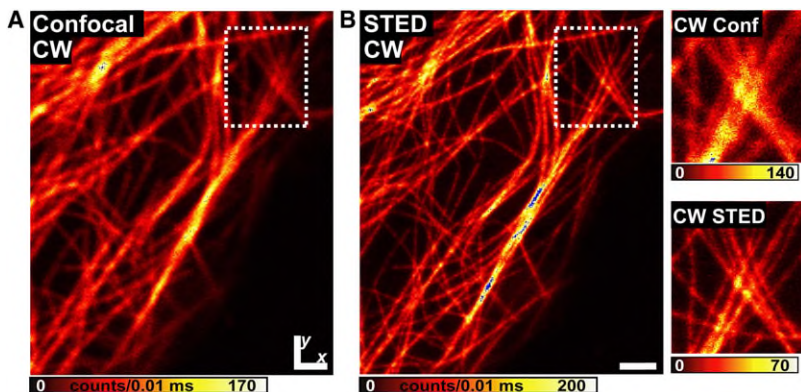


FIGURE 4 Continuous wave (CW) STED imaging of tubulin-associated protein MAP2 labeled with hAGT-TMR. The magnifications point out the superior resolution obtainable through CW STED that simplifies the setup compared to the pulsed STED approach. Single tubules can be distinguished in the STED image, whereas in the confocal counterpart, they seem to form bundles. Scale bar = 1  $\mu\text{m}$ .

Next, we imaged the distribution of caveolin1 (CAV1) in living cells. CAV1 is involved in receptor independent endocytosis (27). We find that CAV1 forms clusters on the plasma membrane, which are clearly better resolved in the STED than in the corresponding confocal image. As is the case with vimentin, the images obtained with Citrine as a fusion label are comparable to those obtained with hAGT/TMR-Star.

The data shown thus far were imaged using pulsed lasers. Because the most complex and expensive part of the STED microscope is the STED laser consisting of a Ti:Sapphire laser and OPO, we explored whether labeling with hAGT/TMR-Star is viable when using continuous wave (CW) lasers for both excitation and STED (16,28). In this case, the setup is greatly simplified because pulse synchronization and stretching is obsolete. Concretely, a 532-nm CW laser diode (Dual Calypso, Cobolt, Sweden) was used for excitation, whereas the STED light of 647 nm was provided by a Krypton laser (Innova, Coherent, CA). Otherwise, the microscope setup was the same as for the pulsed mode. The focal power of the CW STED beam was 236 mW, yielding an intensity  $I = 130 \text{ MW/cm}^2$  at the doughnut crest. Note that in the CW case, depending on the lifetime of the fluorescent state (28),  $I$  is lower by a factor of 8–10 with respect to the 300 ps pulsed mode, as is  $I_s$ . Fig. 4 shows living PtK2 cells expressing the microtubule associated protein MAP2 (29) fused to hAGT labeled with TMR-Star. The CW-STED image (Fig. 4 B) shows individual microtubules, which cannot be separated in the confocal reference image (Fig. 4 A). When using a pulsed laser, images of similar brightness and resolution can be obtained. This example shows that a cost-efficient and rugged CW STED microscope is capable of carrying out live cell studies using a sufficiently stable rhodamine dye.

## DISCUSSION AND CONCLUSION

A distinct advantage of a labeling procedure such as hAGT is that it offers, in principal, an unlimited range of substrates. In particular, cell-permeable substrates offer covalent labeling of proteins in the interior of living cells. Although only

slightly smaller in size than autofluorescent proteins, hAGT is, to our knowledge, the smallest tagging protein currently available capable of intracellular covalent binding of virtually any fluorophore. Further developments of the tag should decrease its size, thus also decreasing its potential interference with protein function. Using smaller labels also becomes increasingly more important with improving resolution.

Fusion proteins of hAGT can be specifically labeled with benzylguanines carrying a label at the 4' position. The concomitant self-labeling reaction is highly specific. On incubation with the substrate, a stable covalent thioether bond is formed between the protein and the label, ensuring chemical stability of the label for long-term experiments. There is no basic limitation to the nature of the label. Besides organic fluorophores, other molecules can be used as well. Membrane permeability, toxicity, and background are likely to pose initial restraints, however, and have to be considered when selecting the fluorophore. On the other hand, because the chemical synthesis of the substrate is a straightforward one-step reaction between the NHS-ester of the label and the linker, a large number of dyes can be explored readily.

Compared to FP-labeling, a drawback of this type of labeling is the requirement of extra staining and washing steps, which last for  $\sim 30$  min. To minimize the background and to optimize the signal, the labeling procedure has to be adapted for the special needs, which is more elaborate than working with FPs. On the other hand, the nature of the labeling mechanism also allows dedicated biological experimental procedures, such as pulse-chase experiments, where proteins are distinguished in different points in time.

A tetramethylrhodamine derivative was used as a substrate for hAGT, because rhodamines are relatively photostable and commercially available. Compared to the yellow fluorescent protein Citrine, which was used recently to image the endoplasmic reticulum of a living cell by STED microscopy, the tetramethylrhodamine-derivative offers absorption and emission spectra that are favorably red-shifted by  $\sim 50$  nm. The viability of STED nanoscopy with these labels is reflected by the fact that the obtained resolution (40 nm) is the highest resolution reported so far in the interior of a living cell, and also by the fact that movies with  $>10$  frames at

50 nm resolution could be recorded before photobleaching. Because fluorophore diffusion is largely precluded due to the covalent attachment to a site specific protein, potentially bleached fluorophores could not have been replenished by fresh labels, which again speaks for their photostability under STED imaging conditions. The compatibility with continuous wave STED microscopy should also facilitate the implementation of this contrast mode.

We believe the labeling approach presented in this study has the potential to substantially expand the scope of STED imaging of live cells to a broader range of samples and questions. The freedom of choosing hAGT-substrates also prepares the ground for multicolor live-cell STED imaging. Simultaneous tagging with GFP and its derivatives should also allow colocalization studies without severe crosstalk. Other self-labeling protein tags could also be used for colocalization. In particular, a close analog to hAGT is available, referred to as CLIP-tag, which reacts with parasubstituted benzyl cytosines. This enables free choice of a pair of compatible dyes for two-color STED imaging. In addition to using a different fluorophore, another interesting avenue is to attach two or multiple dye molecules to a single protein tag; hence, brightness and bleaching kinetics could be substantially improved.

In summary, we have shown that using the self-labeling protein hAGT in conjunction with the rhodamine dye TMR as a substrate is a versatile labeling strategy for STED microscopy using both pulsed and CW lasers, which significantly expands the application range of far-field fluorescence nanoscopy of living cells.

## SUPPORTING MATERIAL

A movie is available at [http://www.biophysj.org/biophysj/supplemental/S0006-3495\(09\)01567-7](http://www.biophysj.org/biophysj/supplemental/S0006-3495(09)01567-7).

We thank T. Gilat for technical assistance, J. Jethwa for critical reading of the manuscript, and A. Schönle for support with the software ImSpector.

This work was supported by the German Ministry for Research and Education (BMBF, Biophotonik III) and by a Gottfried-Wilhelm-Leibniz Award of the Deutsche Forschungsgemeinschaft (to S.W.H.).

## REFERENCES

1. Tsien, R. Y. 2003. Imagining imaging's future. *Nat. Rev. Mol. Cell Biol.* Suppl:SS16–SS21.
2. Born, M., and E. Wolf. 2002. Principles of Optics. Cambridge University Press, Cambridge, New York, Melbourne, Madrid, Cape Town.
3. Fernandez-Suarez, M., and A. Y. Ting. 2008. Fluorescent probes for super-resolution imaging in living cells. *Nat. Rev. Mol. Cell Biol.* 9:929–943.
4. Hell, S. W. 2007. Far-field optical nanoscopy. *Science*. 316:1153–1158.
5. Zhuang, X. 2009. Nano-imaging with STORM. *Nat. Photonics*. 3: 365–367.
6. Hell, S. W., and J. Wichmann. 1994. Breaking the diffraction resolution limit by stimulated-emission: stimulated-emission-depletion fluorescence microscopy. *Opt. Lett.* 19:780–782.
7. Klar, T. A., S. Jakobs, ..., S. W. Hell. 2000. Fluorescence microscopy with diffraction resolution barrier broken by stimulated emission. *Proc. Natl. Acad. Sci. USA*. 97:8206–8210.
8. Dyba, M., and S. W. Hell. 2002. Focal spots of size  $\lambda/23$  open up far-field fluorescence microscopy at 33 nm axial resolution. *Phys. Rev. Lett.* 88:163901.
9. Willig, K. I., S. O. Rizzoli, ..., S. W. Hell. 2006. STED microscopy reveals that synaptotagmin remains clustered after synaptic vesicle exocytosis. *Nature*. 440:935–939.
10. Hell, S. W. 2003. Toward fluorescence nanoscopy. *Nat. Biotechnol.* 21: 1347–1355.
11. Westphal, V., and S. W. Hell. 2005. Nanoscale resolution in the focal plane of an optical microscope. *Phys. Rev. Lett.* 94:143903.
12. Betzig, E., G. H. Patterson, ..., H. F. Hess. 2006. Imaging intracellular fluorescent proteins at nanometer resolution. *Science*. 313:1642–1645.
13. Rust, M. J., M. Bates, and X. W. Zhuang. 2006. Sub-diffraction-limit imaging by stochastic optical reconstruction microscopy (STORM). *Nat. Methods*. 3:793–795.
14. Hess, S. T., T. P. K. Girirajan, and M. D. Mason. 2006. Ultra-high resolution imaging by fluorescence photoactivation localization microscopy. *Biophys. J.* 91:4258–4272.
15. Westphal, V., S. O. Rizzoli, ..., S. W. Hell. 2008. Video-rate far-field optical nanoscopy dissects synaptic vesicle movement. *Science*. 320:246–249.
16. Hein, B., K. I. Willig, and S. W. Hell. 2008. Stimulated emission depletion (STED) nanoscopy of a fluorescent protein-labeled organelle inside a living cell. *Proc. Natl. Acad. Sci. USA*. 105:14271–14276.
17. Shroff, H., C. G. Galbraith, ..., E. Betzig. 2008. Live-cell photoactivated localization microscopy of nanoscale adhesion dynamics. *Nat. Methods*. 5:417–423.
18. Tsien, R. Y., L. Ernst, and A. Waggoner. 2006. Fluorophores for confocal microscopy: photophysics and photochemistry. In *Handbook of Biological Confocal Microscopy*. J. B. Pawley, editor. Springer, New York. 338–352.
19. Griffin, B. A., S. R. Adams, and R. Y. Tsien. 1998. Specific covalent labeling of recombinant protein molecules inside live cells. *Science*. 281:269–272.
20. Los, G. V., L. P. Encell, ..., K. V. Wood. 2008. HaloTag: a novel protein labeling technology for cell imaging and protein analysis. *ACS Chem. Biol.* 3:373–382.
21. George, N., H. Pick, ..., K. Johnsson. 2004. Specific labeling of cell surface proteins with chemically diverse compounds. *J. Am. Chem. Soc.* 126:8896–8897.
22. Keppler, A., S. Gendreizig, ..., K. Johnsson. 2003. A general method for the covalent labeling of fusion proteins with small molecules in vivo. *Nat. Biotechnol.* 21:86–89.
23. Liu, H., M. Xu-Welliver, and A. E. Pegg. 2000. The role of human O-6-alkylguanine-DNA alkyltransferase in promoting 1,2-dibromoethane-induced genotoxicity in *Escherichia coli*. *Mutat. Res.* 452:1–10.
24. Lamesch, P., N. Li, ..., M. Vidal. 2007. hORFeome v3.1: a resource of human open reading frames representing over 10,000 human genes. *Genomics*. 89:307–315.
25. Goodenough, D. A., J. A. Goliger, and D. L. Paul. 1996. Connexins, connexons, and intercellular communication. *Annu. Rev. Biochem.* 65:475–502.
26. Godsel, L. M., R. P. Hobbs, and K. J. Green. 2008. Intermediate filament assembly: dynamics to disease. *Trends Cell Biol.* 18:28–37.
27. Rothberg, K. G., J. E. Heuser, ..., R. G. Anderson. 1992. Caveolin, a protein component of caveolae membrane coats. *Cell*. 68:673–682.
28. Willig, K. I., B. Harke, ..., S. W. Hell. 2007. STED microscopy with continuous wave beams. *Nat. Methods*. 4:915–918.
29. Dehmelt, L., and S. Halpain. 2005. The MAP2/Tau family of microtubule-associated proteins. *Genome Biol.* 6:204.